

# Pilot-Symbols Aided Carrier Phase Recovery for 100G PM-QPSK Digital Coherent Receivers

Maurizio Magarini<sup>1</sup>, Luca Barletta<sup>1</sup>, Arnaldo Spalvieri<sup>1</sup>, Timo Pfau<sup>2</sup>, Francesco Vacondio<sup>3</sup>, Marianna Pepe<sup>4</sup>, Marco Bertolini<sup>4</sup> and Giancarlo Gavioli<sup>4</sup>

<sup>1</sup> Dipartimento di Elettronica e Informazione, Politecnico di Milano, Italy

<sup>2</sup> Alcatel-Lucent Bell Labs, Nozay, France

<sup>3</sup> Alcatel-Lucent Bell Labs, Murray Hill, USA

<sup>4</sup> Alcatel-Lucent Italia, Vimercate, Italy

*A feed-forward pilot-symbols aided carrier phase recovery scheme is described. The approach relies on pilot symbols that are time-division multiplexed with the transmitted data. The main advantage of the proposed solution is that of avoiding the phase ambiguity problem after a cycle slip. For homogeneous PM-QPSK transmission the proposed scheme outperforms blind carrier recovery with differential decoding.*

## 1. Introduction

Investigation of advanced modulation schemes and forward error correcting (FEC) codes which better suit the characteristics of the optical channel, together with coherent digital signal processing (DSP) at the receiver, is a key issue to enable long-haul transmission at high bit-rates [1]. Due to implementation constraints, DSP operations in real time demonstrators of coherent receivers are based on non-data aided, or blind, feed-forward equalization and synchronization algorithms [2]. One of the most critical aspects in the design of such receivers is represented by the low tolerance of high order modulations to carrier phase noise [3].

Several feed-forward blind carrier phase recovery schemes for quadrature amplitude modulation (QAM) constellations with  $M$  points have been proposed for efficient hardware implementation. The most wide-spread approaches are derived from modifications of the  $M$ -power synchronizer [4]. However, better performance can be achieved if the approximated maximum likelihood (ML) criterion of [3] is adopted. As is known, the performance of feed-forward blind algorithms is susceptible to phase errors that are inherent in the carrier phase estimation process [5]. The dominant source of performance degradation is represented by cycle slips, which consist in temporary losses of synchronism of the carrier phase recovery circuit induced by low signal-to-noise ratio (SNR) and/or large phase noise conditions at which the receiver must operate [5]. Due to the four-fold rotational symmetry of the QAM constellation, the recovered phase after a cycle slip may differ of an integer multiple of  $\pi/2$  from the true carrier phase. This problem is commonly tackled by differentially encoding the bits associated with the constellation points. However, the use of differential decoding leads to receiver sensitivity penalties that become more evident for coded transmission [6].

An approach to avoid the differential decoding is here proposed that is based on a periodic insertion of time-division multiplexed pilot symbols [7]. Pilot symbols provide the carrier phase recovery circuit with known symbols at some fixed position. The impact of the pilot rate is investigated by using experimental data for a long-haul 100 Gb/s polarization-multiplexed (PM) quadrature phase shift keying (QPSK) wavelength-division multiplexing (WDM) signal in different transmission scenarios. A comparison of the performance between the proposed and the blind approximated ML criterion scheme, in terms of net coding gain (NCG) and SNR loss with respect to coherent detection, is carried out.

## 2. Experimental set-up

The experimental setup used for signal generation is shown in Fig. 1(a). A distributed-feedback laser at 1545 nm with a linewidth of  $\Delta f = 1$  MHz was modulated using an integrated dual-polarization nested Mach-Zehnder modulator to generate a 100 Gb/s PM-QPSK signal. Two WDM transmission configurations were tested; in the hybrid transmitter configuration the test channel is wavelength multiplexed with 79 non-return-to-zero (NRZ) channels modulated at 10 Gb/s spaced at 50 GHz; in the homogeneous transmitter configuration the test channel is multiplexed with 79 PM-QPSK 100Gb/s channels spaced at 50 GHz. The signal was then launched into the recirculating loop depicted in Fig. 1(b). Two different link scenarios were investigated; in the first the loop span is 3x100 km of compensated standard single mode fiber (SSMF); in the second the loop span is 4x75 km of

compensated non-zero dispersion shifted fiber (NZDSF). A dispersion compensation fiber (DCF) was used between the two-stage EDFA, according to a dispersion map for typical terrestrial systems [8].

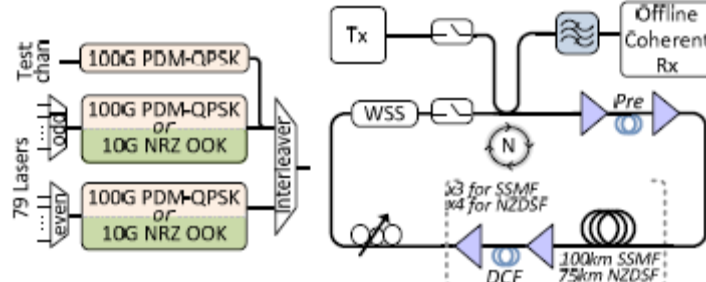


**Fig. 1: Experimental set-up for generation, transmission and coherent detection of 100 Gb/s PM-QPSK homogeneous and hybrid WDM signals**

The maximum reach at bit error rate (BER) target lower than  $2 \cdot 10^{-2}$  for homogeneous WDM transmission was found to be 6 SSMF loops and 5 NZDSF loops, while for hybrid WDM transmission was found to be 5 SSMF loops and 3 NZDSF loops. The launch powers into the SSMF and NZDSF were -1 dBm/channel and -3dBm/channel for the homogeneous case and -2 dBm/channel and -7 dBm/channel for the hybrid case, respectively. Note that a target input BER in the order of  $10^{-2}$  is usually considered for soft-decision decoding [6]. At the receiver, the signal was selected detected with a standard digital coherent receiver as described in [9].

### 3. Pilot-symbols aided carrier phase recovery

As shown in [10], for the experiments considered in Sec. 2 the  $k$ -th sample of the discrete time received signal at the input of the carrier phase recovery circuit can be modeled as:

$$x_k = a_k \cdot e^{j\theta_k} + n_k, \quad (1)$$

where  $\{a_k\}$  is the unitary average power symbol sequence, including payload and pilot symbols and  $\{n_k\}$  is a zero mean complex additive white Gaussian noise (AWGN) sequence with variance  $\text{SNR}^{-1}$ . The unknown time-varying phase-noise sequence  $\{\theta_k\}$  of the incoming carrier is a Wiener process defined by the value of linewidth times symbol duration  $\Delta f \cdot T$  (we follow the same characterization of [3] of the phase-noise model). Blind carrier frequency estimation according to [11] is implemented to remove any residual frequency offset in (1). Let the pilot-rate be  $M^{-1}$ , meaning that one pilot symbol is periodically inserted after  $M-1$  payload symbols. Without losing generality, we assume that the  $i$ -th pilot symbol occurs at the discrete time instant  $iM$ , hence the pilot sequence is a zero-padded sequence given by:

$$p_k = \begin{cases} a_k, & k = iM \\ 0, & k \neq iM. \end{cases} \quad (2)$$

Time synchronization of pilot symbols is obtained by correlating the received sequence with the pilot sequence. The block diagram of the phase synchronization system proposed in this work is shown in Fig.2. A coarse phase tracking based on pilot symbols is done in the first stage. The received sequence in (1) is multiplied with the complex conjugate of the zero-padded pilot sequence given in (2) and the resulting sequence is filtered by an interpolation filter that is optimized as described in [7]. The phase correction is generated by taking the argument of the samples at the output of the interpolation filter. Blind phase estimation based on the approximated ML algorithm of [3] with 16 test carrier phases then follows to correct the residual phase offset.

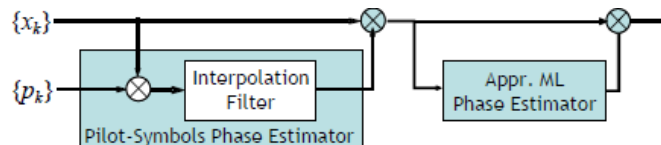


**Fig. 2: Block diagram of the proposed two-stage pilot-symbols aided carrier phase estimator**

A major difference occurs between our implementation and that of [3] and, in general, of other blind algorithms. Since the pilot-symbols aided phase estimator relies on an absolute reference of phase provided by pilot symbols, the correction it provides does not suffer of any phase ambiguity. This means that the sequence at the input of the second stage approximated ML estimator is

assumed to be subject only to a small phase offset and the phase estimate it produces is limited to the range  $[-\pi/4, \pi/4]$ . Therefore, no unwrapping is required and no cycle slips are introduced by the proposed scheme.

#### 4. Experimental results

The Q-factor at maximum distance is evaluated both for the receiver based on approximated ML blind phase estimation and differential decoding and for the proposed pilot-symbols aided phase estimation algorithm and coherent detection. At maximum reach the pilot-rate is varied and the impact on the Q-factor assessed. Results obtained in different transmission scenarios are shown in Table I.

TABLE I  
MEASURED Q-FACTOR FOR PILOT-SYMBOLS AIDED PHASE ESTIMATION AND FOR BLIND APPROXIMATED ML ESTIMATION IN DIFFERENT SCENARIOS

	Q-factor (dB)				Reach (loops)
	Pilot-symbols aided			Blind appr. ML	
	3%	5%	10%		
NZDF Hybrid	6.5	7	7.4	6.1	3
NZDF Homog.	7.2	7.2	7.2	6	5
SSMF Hybrid	6.4	7	7.3	6.2	5
SSMF Homog.	7.3	7.3	7.3	6	6

The difference of performance between homogeneous and hybrid transmission can be explained by observing that the homogeneous transmission cases are characterized by linewidth times symbol durations in the order of  $\Delta f \cdot T \gg 4 \cdot 10^{-4}$  while for the hybrid cases higher values in the order of  $10^{-3}$  were found [10]. Due to the errors introduced by differential decoding, the Q-factor measured for pilot-symbols aided phase estimation with coherent demodulation is higher than that for blind phase estimation with differential decoding. The results shown in Table I for pilot-symbols aided phase estimation do not yet include the penalties expected in SNR and in NCG associated with the different pilot-rates.

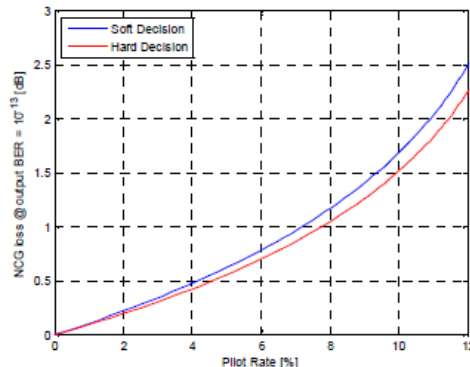


Fig. 3: NCG loss with respect to pilot-rate for hard and soft decision FEC for a reference overhead of 16%

Assuming a fixed information bit-rate, the introduction of pilot-symbols reduces the overhead available for FEC which, in turn decreases the NCG. An FEC with a fixed overhead of 16%, code rate  $R = 0.86$ , is studied. This code rate, considered in [6], allow both for concatenation with an outer code and for having room for a practical range of pilot-rates. Fig. 3 shows the NCG loss at output BER of  $10^{-13}$  for coherent detection versus the increase of pilot-rate, computed considering the SNR associated to the QPSK constrained capacity [6]. The Figure shows the NCG loss with respect to the pilot-rate expressed in terms of percentage of the bit-rate, for both hard and soft decision decoding. At the considered rate, soft decision decoding with infinite quantization provides an improvement up to 1.26 dB in NCG compared to hard decision decoding [6]. The introduction of pilot symbols increases the required SNR for a given BER target. Since pilot symbols do not carry information, the cost associated to them can be expressed directly in terms of SNR loss compared to the case where they are not introduced. The overall penalty, defined as the sum of the SNR and NCG losses, is summarized in Table II for three different pilot-rate values. Taking into account the pilot symbols penalty on the measured Q-factor of Table I, the estimate of SNR penalty for pilot-symbols aided phase estimation at different pilot-rates with respect to coherent demodulation for the different scenarios is shown in Fig. 4. The SNR loss of differential decoding with respect to coherent detection

at the target BER of  $2 \cdot 10^{-2}$  is 1.2 dB. For scenarios with limited phase noise, i.e. homogeneous transmission, the use of pilot symbols requires low insertion rate below 5%.

TABLE II  
NCG AND SNR LOSS FOR SOFT DECISION DECODING VS. PILOT-RATE.

Pilot-rate	SNR loss (dB)	NCG loss wrt coherent (dB)	Pilot symbols penalty (dB)
10%	0.45	1.68	2.13
5%	0.22	0.62	0.84
3%	0.13	0.34	0.47

For scenarios with strong phase noise, such as hybrid transmission, a higher pilot-rate is required and the performance is comparable to that of approximate ML blind phase estimation followed by differential decoding. Note that for hard decision decoding a target BER in the order of  $10^{-3}$  is usually considered, that corresponds to a higher SNR working point. Phase noise effects are less severe at higher SNR and a lower pilot rate is therefore required. However, also the penalty of differential decoding is reduced and the performance of the two carrier recovery schemes needs to be evaluated.

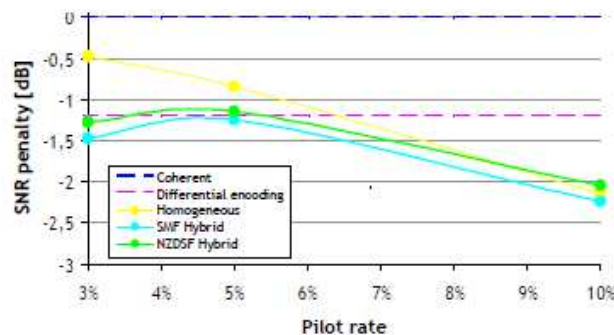


Fig. 4: SNR penalties with respect to coherent demodulation measured at maximum reach for pilot-symbols aided phase estimation with different pilot-rates and over the different experimental scenarios

## 5. Conclusions

Pilot-symbols aided carrier phase estimation is proposed. Its performance is experimentally investigated in case of long-haul transmission of a 100Gb/s PM-QPSKWDM signal in different propagation scenarios. The proposed scheme does not introduce cycle slips and avoids differential decoding. We show that in case of homogeneous PMQPSK transmission the proposed scheme outperforms blind phase estimation with differential decoding while in presence of highly nonlinear transmission, as for hybrid NRZ-PM-QPSK transmission, the performance is comparable.

**ACKNOWLEDGMENTS** The authors would like to thank D. Di Mola and L. Razzetti from Alcatel-Lucent Optics Division and Y. Chen at Bell Labs for support and P. Winzer, X. Liu, S. Chandrasekhar at Bell Labs for useful discussion on this work.

## References

- [1] I. B. Djordjevic, M. Arabaci, L. L. Minkov, "Next generation FEC for high-capacity communication in optical transport networks," *J. Lightw. Technol.*, vol. 27, pp. 3518-353, Aug. 2009.
- [2] R. Noe, U. Ruckert, S. Hoffmann, R. Peveling, T. Pfau, M. El-Darawy, A. Al-Bermani, "Real-time implementation of digital coherent detection", in *Proc. of Europ. Conf. Opt. Commun. (ECOC)*, Vienna, Austria, 2009, paper 5.4.3.
- [3] T. Pfau, S. Hoffmann, R. Noe, "Hardware-efficient coherent digital receiver concept with feedforward carrier recovery for M-QAM constellations," *J. Lightw. Technol.*, vol. 27, pp. 989-999, Apr. 2009.
- [4] I. Fatadin, D. Ives, S. J. Savory, "Laser linewidth tolerance for 16-QAM coherent optical systems using QPSK partitioning," *IEEE Photon. Technol. Lett.*, vol. 22, pp. 631-633, May 2010.
- [5] U. Mengali, A. N. D'andrea, *Synchronization Techniques for Digital Receivers*, Plenum Press Ed., 1997. [6] T. Mizuochi, Y. Miyata, K. Kubo, T. Sugihara, K. Onohara, H. Yoshida, "Progress in soft-decision FEC," in *Proc. of Opt. Fiber Commun. Conf. (OFC)*, Los Angeles, CA, 2011, NWC2.
- [7] A. Spalvieri, L. Barletta, "Pilot-aided carrier recovery in the presence of phase noise," *IEEE Trans. Commun.*, vol. 59, pp. 1966-1974, July 2011.
- [8] J.-C. Antona, M. Lefrançois, S. Bigo, G. Le Meur, "Investigation of advanced dispersion management techniques for ultra-long haul transmissions," in *Proc. of Europ. Conf. Opt. Commun. (ECOC)*, Glasgow, Scotland, 2005, Mo.3.2.6.
- [9] S. Savory, G. Gavioli, R. I. Killey, P. Bayvel, "Electronic compensation of chromatic dispersion using a digital coherent receiver," *Opt. Exp.*, vol. 15, pp. 2120-2126, Feb. 2007.
- [10] M. Magarini, A. Spalvieri, F. Vacondio, M. Bertolini, M. Pepe, G. Gavioli, "Empirical modeling and simulation of phase noise in longhaul coherent optical transmission systems," *Opt. Exp.*, vol. 19, pp. 22455-22461, Nov. 2011.
- [11] A. D'Amico, A. D'Andrea, R. Regiannini, "Efficient non-data-aided carrier and clock recovery for satellite DVB at very low signal-to-noise ratios," *IEEE J. Sel. Areas Commun.*, vol. 19, 2001, pp. 2320-2330.